International Journal of Engineering and Technical Research (IJETR)
ISSN: 2321-0869 (O) 2454-4698 (P), Volume-13, Issue-1, January-June 2023

Femtosecond pulse laser irradiation of gold/nickel/chromium triple-layer metal film: The results of two-temperature model simulations

M. Saghebfar, S. Momeni, S. Nazem

***Abstract*— In this work, the results of computational single-shot laser pulse irradiation of gold/nickel/chromium metal film using two-temperature model are presented. The thermal response of Au/Ni/Cr triple-layer film is investigated after femtosecond laser pulse irradiation with pulse duration $30\,fs$ and $800\,nm$ laser wavelength in submelting condition by introducing the ideal interface between gold/nickel and nickel/chromium layers. The excited electrons on the first upper layer couples effectively with lattice and the lattice temperature jump at the interface between gold/nickel and nickel/chromium layers. The role of various lengths of first gold layer and specified thickness of last chromium layer is also studied in detail. Interface overheating increases for thinner thicknesses of first Au layer and the electron-phonon coupling factor is the most effective parameter in overheating at interface. The simulated results provide more information about heat propagation from femtosecond laser irradiation of multi-layer metal films.**

***Index Terms*— Femtosecond pulse laser, interface overheating, gold/nickel/chromium metal film, two-temperature model**

I. INTRODUCTION

It is possible to produce powerful femtosecond laser systems with the development of ultrashort lasers based on chirped pulse amplification [1], which are widely used in a variety of fields including material processing [2], pulsed-laser deposition [3], material micromachining, element analysis, and the understanding of fundamental physical processes [4,5]. Thus, it is important to understand the physical characteristics of femtosecond laser-mater interaction. Among these materials, the femtosecond laser-induced irradiation of multi-layer metal films is a challenging research topic because of many applications in variety of fields [6-8]. During ultrashort laser-metal interaction, the laser energy is first deposited into electrons on the metal surface and the energy transport process in heating of thin films consists of two stages [9,10]. The first stage is the absorption of the laser energy through photon-electron interactions within the ultrashort pulse duration. It takes a few femtoseconds for electrons to reestablish the Fermi distribution. The second stage is the energy distribution to the lattice through electron-phonon interactions, typically on the order of a few tens of picoseconds.

Mohammd Saghebfar, Optics-Laser Science and Technology Research Center, Malek Ashtar University, Isfahan, Iran.
Samira Momeni, Physics Department, Isfahan University, Isfahan, Iran,.
Saeed Nazem, Physics Department, Isfahan University, Isfahan, Iran.

Recently, many researchers presented micro or nanoscale heat transfer models to analyze the thermal nonequilibrium in thin metallic film and conducted the experiments of ablation for thin metallic films [11-16]. Among these theoretical models, the two-temperature model (TTM) has been widely used to examine electron-phonon interactions and nonequilibrium energy transport in metallic thin films [17-25]. Compared to long pulsed lasers, ultrashort-pulsed lasers enable users to precisely control the size of the heat-affected zone, the heat rate, and the interfacial velocity [26]. When laser pulse duration is much bigger than the time necessary for electronic and phononic subsystems to reach the equilibrium, $\tau_{laser} >> \tau_{eq}$, the dynamics of the temperature can be reliably well described by only one temperature model, where there is no distinction between electronic and phononic temperatures and carrier concentration can be determined by Fermi-Dirac distribution. But if laser pulse duration is less or comparable with the time of temperature equilibration, $\tau_{laser} \leq \tau_{eq}$, one temperature model is no longer adequate for describing of the thermal properties of the system, that is why the TTM is widely used to explain carrier dynamics in femtosecond optical studies [18,27-29]. The multi-layer system can well serve as the ideal structure for satisfying the thermal, optical and electronic requirements in development of MEMS, photoelectric equipment and biochips [30-32] and important components in many microelectronic devices. Thus, the transportation of thermal energy through thin films is of vital importance in micro-technological applications. Exploration of temperature-dependent thermal properties is necessary to advance our fundamental understanding of ultrafast heat transportation. In fact, in multi-layer system upper layer is illuminated by a normally incident ultrashort laser pulse and the energy of laser pulse is partially transferred to free electrons within the skin layer and the remaining part is reflected according to the reflection coefficient of first layer. Excited free electrons diffuse with velocities close to the Fermi velocity and penetrating on hundreds of nanometers in case of noble metals [33-35]. The length of diffusion is determined by thermal conductivity, k, and electron-phonon coupling coefficient, g, giving $\delta_{diff} = \sqrt{k/g}$. The thermalization dynamics across the interface of layers trends to be even more complex compared to that of conventional ultrafast laser excitation.

In this work, the TTM simulation results of femtosecond laser pulse irradiation of gold/nickel/chromium metal film are presented. First, the spatial variations of electron and lattice temperature in each layer after laser pulse irradiation is studied. Then, the effect of each layer thickness is

investigated on the interface overheating. We take advantage of a theoretical method to find the distribution of heat in a triple-layer of Au/Ni/Cr metal structure.

II. Mathematical Model

A. *Two-temperature model for triple-layer thin film*

As mentioned in introduction, the theoretical method to investigate the ultrashort laser-matter interaction is the two-temperature model. The two-temperature model describes the temporal and spatial evolution of the lattice and electrons temperatures in the irradiated metal. In ultrafast laser heating of metals, a transient nonequilibrium occurs between the effective electron temperature, and the effective lattice temperature, due to the small heat capacity of the electrons. The laser energy is first absorbed by electrons owing to the inverse bremsstrahlung and free electron is heated to larger kinetic energy during several femtoseconds. It is followed by a fast energy relaxation within the electron subsystem, thermal diffusion, and an energy transfer to the lattice owing to the electron-phonon coupling. The one-dimension TTM, initially proposed by Anisimov et al. [36], is given below:

$$C_e\frac{\partial T_e}{\partial t} = \nabla.\{k_e \nabla T_e\} - g(T_e - T_l) + S(z,t) \quad (1)$$

$$C_e\frac{\partial T_e}{\partial t} = \nabla.\{k_e \nabla T_e\} - g(T_e - T_l) + S(z,t) \quad (2)$$

Where C_e and C_l are the electron and lattice heat capacities respectively, k_e is the electron thermal conductivity, g is the electron-phonon coupling coefficient and S is the laser heating source function as [37]:

$$S = \frac{0.94J}{\tau_p \delta}(1-R)\, exp\left[\frac{-z}{\delta} - 2.77\left(\frac{t}{\tau_p}\right)^2\right] \quad (3)$$

Here δ can be identified as the optical penetration depth, J is the laser fluence in (J/m^2), τ_p is the femtosecond pulse duration and R is the reflectivity of the sample. For these calculations, the value of $C_e = \gamma T_e$ where γ is the Sommerfeld parameter is used. The temperature-dependent values of the electron thermal conductivity k_e, and electron-phonon coupling coefficient g was calculated using the following expressions [38-39]:

$$k_e = k_{e0}\frac{T_e}{\frac{A_e}{B_l}T_e^2 + T_l} \quad (4)$$

$$g = G_0\left(\frac{A_e}{B_l}(T_e + T_l) + 1\right) \quad (5)$$

where k_{e0}, A_e and B_l are the material constants and G_0 is the coupling factor at room temperature.

In our work, the results of TTM simulations are performed for the schematic view of the laser heating, which indicates a three-layer metal film with an interface at $z = l_1$ and $z = l_2$, as is shown in Fig. 1.

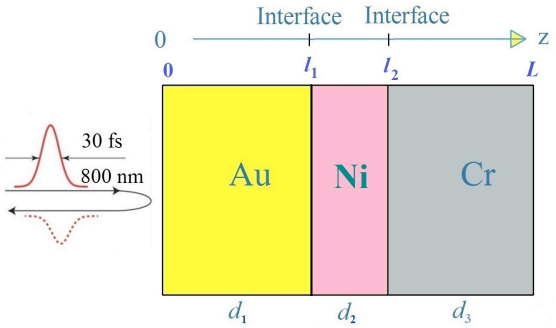

Figure 1: Schematic view of an(a) Au/Ni/Cr triple layer film irradiated with a 30 fs Gaussian laser beam.

We consider that $30\,fs$ laser pulse with wavelength of 800 nm is normally incident at the gold surface. The source term reproduces a Gaussian temporal profile and an exponential attenuation of laser intensity with the depth under the surface. An optical penetration depth of 13.53 nm at a laser wavelength of 800 nm is assumed in the simulations and the absorbed laser fluence, $9\,mJ/cm^2$, is used in the discussion of the simulation results. Other parameters and the physical properties of gold, nickel and chromium, which are used in the model, are listed in Table 1.

Table 1: Gold, nickel and chromium parameters which are used in TTM simulations.

Parameters	Au	Ni	Cr
$G_0(J.m^{-3}.s^{-1}.K^{-1})$	2.3×10^{16}	3.6×10^{17}	4.2×10^{17}
$A_e(s^{-1}.K^{-2})$	1.18×10^{7}	0.59×10^{7}	7.9×10^{7}
$B_l(s^{-1}.K^{-1})$	1.25×10^{11}	1.4×10^{11}	13.4×10^{11}
$C_l(J.m^{-3}.K^{-2})$	2.5×10^{6}	4.1×10^{6}	3.23×10^{6}
$v_F(m.s^{-1})$	1.40×10^{6}	1.82×10^{6}	1.82×10^{6}
$\gamma(J.m^{-3}.K^{-2})$	71	1065	194
$k_{e0}(J.m^{-1}.s^{-1}.K^{-1}$	315	90	95

For the three-layer Au/Ni/Cr thin film, The TTM can be expressed as:

$$C_e^{Au}\frac{\partial T_e^{Au}}{\partial t} = \nabla.\{k_e^{Au}\nabla T_e^{Au}\} - g^{Au}(T_e^{Au} - T_l^{Au}) + S(z,t) \quad (6)$$

$$C_l^{Au}\frac{\partial T_l^{Au}}{\partial t} = \nabla.\{k_l^{Au}\nabla T_l^{Au}\} + g^{Au}(T_e^{Au} - T_l^{Au}) \quad (7)$$

$$C_e^{Ni}\frac{\partial T_e^{Ni}}{\partial t} = \nabla.\{k_e^{Ni}\nabla T_e^{Nir}\} - g^{Ni}(T_e^{Ni} - T_l^{Ni}) \quad (8)$$

$$C_l^{Ni}\frac{\partial T_l^{Ni}}{\partial t} = \nabla.\{k_l^{Ni}\nabla T_l^{Ni}\} + g^{Ni}(T_e^{Ni} - T_l^{Ni}) \quad (9)$$

$$C_e^{Cr}\frac{\partial T_e^{Cr}}{\partial t} = \nabla.\{k_e^{Cr}\nabla T_e^{Cr}\} - g^{Cr}(T_e^{Cr} - T_l^{Cr}) \quad (10)$$

$$C_l^{Cr}\frac{\partial T_l^{Cr}}{\partial t} = \nabla.\{k_l^{Cr}\nabla T_l^{Cr}\} + g^{Cr}(T_e^{Cr} - T_l^{Cr}) \quad (11)$$

In here, since the heat diffusion of the electron subsystem is much faster, so, the thermal conductivity of the lattice is absent as it is negligible in comparison to electron thermal conductivity, and heat diffusion in the lattice system is safely neglected, and the ions therefore only exchange energy locally with the electrons.

The initial conditions to solve the TTM equations for the Au/Ni/Cr triple-layer film are:

$$T_l^{Au}(z,0) = T_e^{Au}(z,0) = 300\,(K) \quad (12)$$

$$T_l^{Ni}(z,0) = T_e^{Ni}(z,0) = 300\,(K) \quad (13)$$

$$T_l^{Cr}(z,0) = T_e^{Cr}(z,0) = 300\,(K) \quad (14)$$

The boundary conditions, neglect heat losses from the front and back surfaces of the sample are:

$$\frac{\partial T_l^{Au}}{\partial z}\Big|_{z=0} = \frac{\partial T_e^{Au}}{\partial z}\Big|_{z=0} = 0 \quad (15)$$

$$\frac{\partial T_l^{Cr}}{\partial z}\Big|_{z=L} = \frac{\partial T_e^{Cr}}{\partial z}\Big|_{z=L} = 0 \quad (16)$$

Finally, the boundary condition at interfaces, $z = l_1$ and $z = l_2$, for the triple-layer metal film can be written as:

$$T_l^{Au}|_{z=l_1} = T_l^{Ni}|_{z=l_1} \quad (17)$$

$$T_e^{Au}|_{z=l_1} = T_e^{Ni}|_{z=l_1} \quad (18)$$

$$k_e^{Au}\frac{\partial T_e^{Au}}{\partial z}\Big|_{z=l_1} = k_e^{Ni}\frac{\partial T_e^{Ni}}{\partial z}\Big|_{z=l_1} \quad (19)$$

$$T_l^{Ni}|_{z=l_2} = T_l^{Cr}|_{z=l_2} \quad (20)$$

$$T_e^{Ni}|_{z=l_2} = T_e^{Cr}|_{z=l_2} \quad (21)$$

$$k_e^{Ni}\frac{\partial T_e^{Ni}}{\partial z}\Big|_{z=l_2} = k_e^{Cr}\frac{\partial T_e^{Cr}}{\partial z}\Big|_{z=l_2} \quad (22)$$

III. Results and Discussion

For numerical solution of two-temperature equations, we considered the ideal interfaces between gold/nickel and nickel/chromium that neglects any kind of electron scattering and performed the simulation of the TTM for the structure of Fig. 1 consisting 150 (nm) of gold layer thickness followed by 20 and 80 (nm) of nickel and chromium layers.

The results of numerical simulation after laser pulse irradiation for electron and lattice temperature for three layers are shown in Fig. 2. As seen from figure, the electron temperature in each layer becomes less than previous layers. But, the lattice temperature for nickel layer has highest value compared to the other two layers. The two-dimensional plots of electron and lattice temperature inside the gold, nickel and chromium layers are also presented in Fig. 2. The fast absorption of $30\,fs$ laser pulse is followed by rapid and deep diffusion of electrons towards the nickel layer. Excited electrons will arrive at the gold/nickel interface by the time of $\approx 107\,fs$,(according to the Fermi velocity and the thickness of gold).

For the first times the concentration of electrons that reached the nickel and chromium layers is low so, the electron temperature in the Ni and Cr layers is very small compared to the gold layer. Within next times the electron temperature in the nickel layer increases and excited electrons after $\approx 118\,fs$ arrives to second interface and then they transfer their energy to the lattice resulting decrease of amplitudes of the electron temperature in all layers.

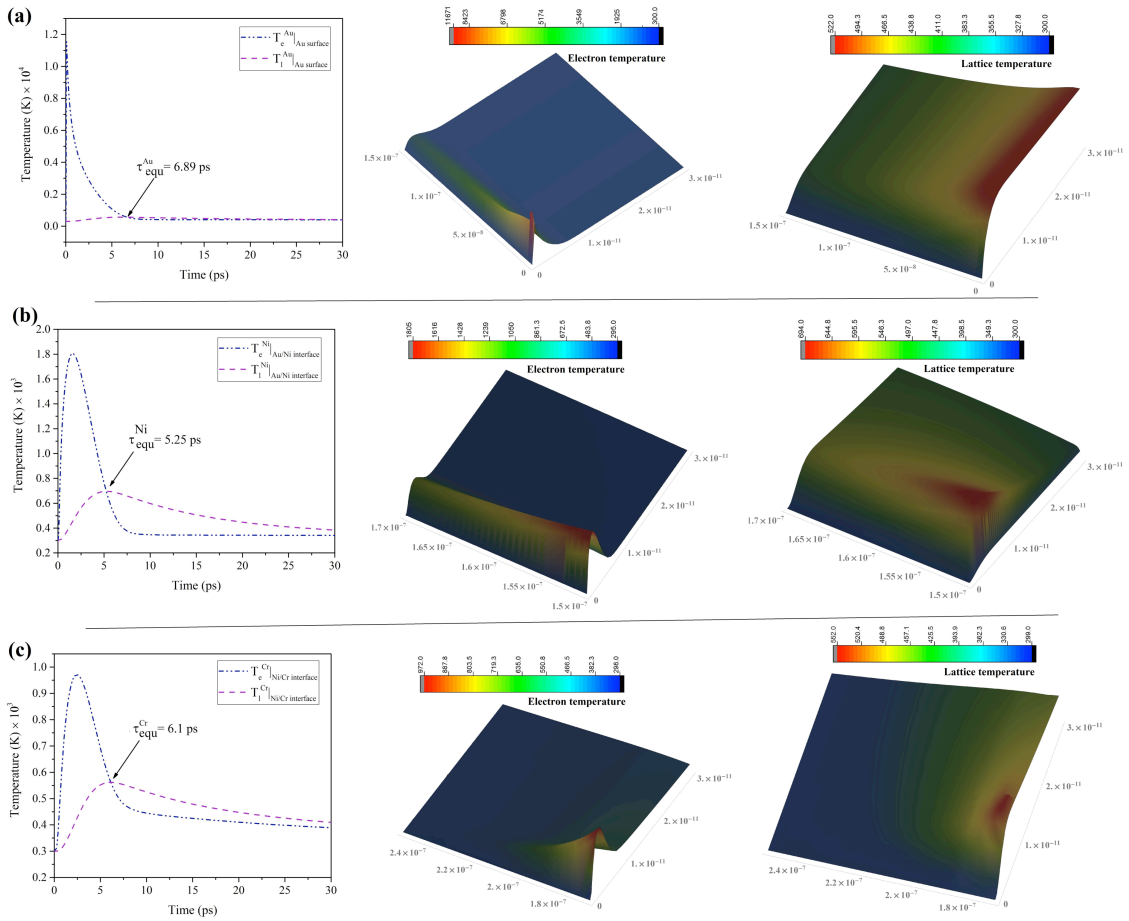

Figure 2: Electron and lattice temperature versus time and spatial variation for gold (a), nickel (b), and chromium (c), layers. $d_1 = 150\ nm$, $d_2 = 20\ nm$, $d_3 = 80\ nm$, $E_{absorbed} = 9\ (mJ/cm^2)$, $\tau_p = 30\ fs$ *and* $800\ nm$ *laser wavelength.*

In order to find the TTM results in various times, the evolution of the lattice and electron temperature at the surface of Au layer and at the interfaces from the nickel side and chromium side versus time are shown in Fig. 3. The nickel and chromium lattice temperature at interface increase rapidly for the time of $5.2\ ps$ and $6.01\ ps$ after $14.5\ ps$,(for Ni), and $10.6\ ps$,(for Cr), these temperatures are equal to the Au surface temperature. The nickel layer lattice temperature is also equal to chromium layer lattice temperature at the time of $20\ ps$ after laser pulse irradiation. It can be seen from Fig. 3 (b) that the maximum electron temperature at gold surface takes place at $0.086\ ps$ and the electron temperature is gradually reduced in subsequent layers. However, dynamics of the electron temperatures show very fast cooling of the electron-gas and reaching equilibrium $8\ ps$ after laser pulse irradiation. In order to understand the dynamic of electron and lattice temperature distributions, the three-dimensional plots of temperatures versus time and position for $150\ nm$, $20\ nm$ and $80\ nm$ thickness of gold, nickel and chromium layers are shown in Fig. 4. According to this figure, due to the discrepancy of the electron phonon coupling constants and lattice heat capacities between these materials, we can see that the lattice

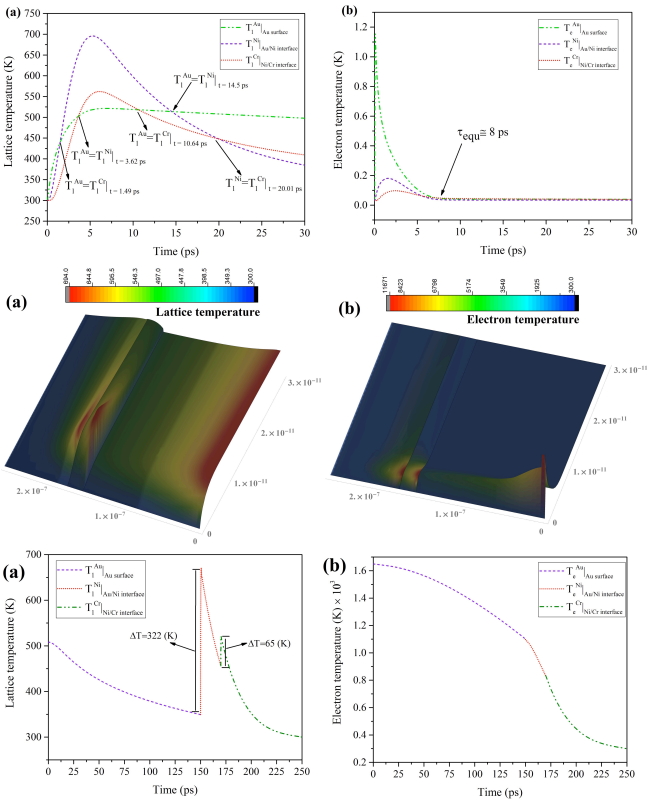

Figure 3: Evolution of the lattice (a), and electron (b), temperature at the Au surface and interfaces from the nickel

side and chromium side versus time for 150, 20 and 80 (nm) thickness of Au, Ni and Cr.

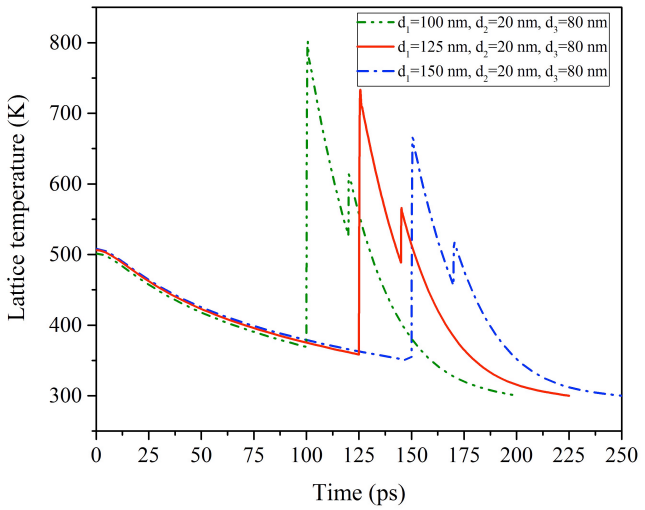

Figure 4: Electron and lattice temperature versus time and spatial variation for gold (a), nickel (b), and chromium (c), layers.

$d_1 = 150\ nm$, $d_2 = 20\,nm$, $d_3 = 80\,nm$, $E_{absorbed} = 9\,(mJ/cm^2)$, $\tau_p = 30\ fs$ *and* $800\ nm$ *laser wavelength.*

overheating at interface depends on the temperature of excited electrons and as the excited electrons on the first upper layer couples effectively with lattice, the lattice temperature jumps at the interface between gold/nickel and nickel/chromium layers.

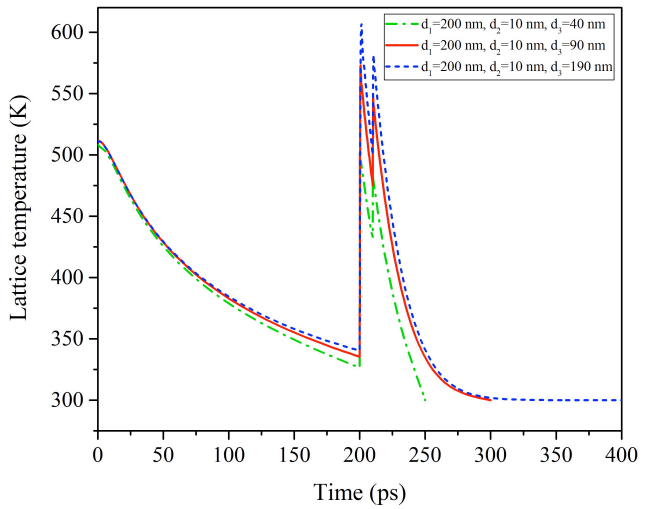

Figure 5: Evolution of the lattice temperature for three thicknesses of chromium layer at the snapshot time of $4\ ps$, *(*$d_1 = 200\ nm$ *and* $d_2 = 10nm$*).*

For more information the lattice and electron temperature along depth at the snapshot time of $4\,ps$ after laser pulse irradiation are presented in Fig. 5. In this case, the value of the nickel and chromium side lattice overheating at the interfaces of Au/Ni and Ni/Cr is 1.92 and 1.49 times respectively for 150 nm thickness of first gold layer. The maximum discrepancy between lattice temperatures in Au/Ni and Ni/Cr interfaces is about $322\ (K)$ and $65\ (K)$. In Fig. 5(b), the value of electron temperature in each layer is less than its value in previous layer.

To see the role of various thickness of first gold layer in chromium overheating at interface we run TTM code for three thicknesses of Au layer. As illustrated in Fig. 2, The values of the nickel and chromium side lattice overheating for $100\ nm$, $125\ nm$ and $150\ nm$ thickness of first gold layer is 2.17, 2.04 and 1.92 times for nickel and 1.67, 1.57 and 1.49 times for chromium respectively. It should be noted that, the thicknesses of nickel and chromium layers in each case is constant. However, it is clear from the results that, the length of first Au layer plays an important role in the value of overheating at the interface and overheating increases for thinner thicknesses of first Au layer.

In here it is useful that, we note to the spatial variation of lattice temperature for different thicknesses of nickel and chromium layers. As presented in Fig. 3, for the specified thicknesses (as shown in figure), the jumping of lattice temperature at Au/Ni and Ni/Cr interfaces for $d_2 = 10\,nm$ thickness of nickel layer compared with previous results, ($d_2 = 20\,nm$), is clearly observed. Moreover, as the thickness of chromium layer moves to larger values, the value of lattice temperature jumping, at interfaces increased. so, in the analysis of heat propagation in multi-layer films, the thickness of all layers affects on the interface overheating and the distribution of lattice and electron temperatures in each layer.

IV. Conclusion

The time evolution and space distribution of temperature in Au/Ni/Cr triple-layer film irradiated by $30\,fs$ pulse laser with a numerical method is performed using the two-temperature model simulations. First, the evolution of the electron and lattice temperature in each layer is presented. Then, the distribution of the electron and lattice temperature at the gold/nickel and nickel/chromium interfaces is described in detail. Based on our findings, the following conclusions can be drawn.

(a) The excited electrons on the first upper layer couples effectively with lattice by the time of $107\ fs$, for $150\ nm$ thickness of gold layer, and the lattice temperature jump at the interface between gold/nickel and nickel/chromium layers. This is due to the fact that, the electron-phonon coupling factor is considerably high for chromium and nickel layers compared to gold, causing the redistribution of the deposited laser energy from the gold side to the nickel and chromium layers.

(b) The electron-phonon coupling factor is the most effective parameter in overheating at interface.

(c) The thickness of first layer play an important role in interface overheating. The distribution of electron temperature around the interface for thicker gold layers is low, so, the lattice overheating at the interface increases for the short thicknesses of first Au layer and, it depends on the snapshot times. For the snapshot times other than $4\,ps$, considered in here, the lattice overheating at interface is different from presented results.

(d) The maximum electron temperature take place inside the gold layer and the electron temperature amplitude in each layer decreases rapidly and equilibrates with the surface temperature $\sim 8\,ps$ after laser pulse irradiation.

(e) A small spatial broadening of lattice heat distribution in nickel and chromium layer is observed due to the increased number of electrons that stayed inside the gold layer close to the gold/nickel and nickel/chromium interface.

V. ACKNOWLEDGEMENTS

The work was supported by Malek Ashtar University, Optics-Laser Science and Technology Research Center.

REFERENCES

[1] D. Strickl and G. Mourou, "Compression of amplified chirped optical pulses'', Opt. Commun. 56, (1985) 219.
[2] T. H. R. Crawford, J. Yamanaka, G. A. Botton and H. K. Haugen, "High-resolution observations of an amorphous layer and sub-surface damage formed by femtosecond laser irradiation of silicon'', J. Appl. Phys. 103, (2008) 053104.
[3] No¨el and J. Hermanna, "Reducing nanoparticles in metal ablation plumes produced by two delayed short laser pulses'', Appl. Phys. Lett. 94, (2009) 053120.
[4] W. Miziolek, V. Palleschi, and I. Schechter, "Laser-induced breakdown spectroscopy (LIBS)'', Camb. Univ. Press, New York, (2006).
[5] C. Phipps, "Laser ablation and its applications'', Springer, New York, (2007).
[6] X. Y. Wang, D. M. Riffe, Y. S. Lee, and M. C. Downer, "Time-resolved electron-temperature measurement in a highly excited gold target using femtosecond thermionic emission'', Phys. Rev. B 50, (1994) 8016-9.
[7] O. Ekici, R. K. Harrison, N. J. Durr, D. S. Eversole, M. Lee and A. Ben-Yakar, "Thermal analysis of gold nanorods heated with femtosecond laser pulses'', J. Phys. D, Appl. Phys. 41, (2008) 185501.
[8] Y. W. Zhang and J. K. Chen, "Ultrafast melting and resolidification of gold particle irradiated by pico-to femtosecond lasers'', J. Appl. Phys. 104 (2008) 054910.
[9] Rethfeld, A. Kaiser, M. Vicanek, and G. Simon, "Ultrafast Dynamics of Nonequilibrium Electrons in Metals under Femtosecond Laser Irradiation'', Phys. Rev. B, 65, (2002) 214303.
[10] D. Y. Tzou, J. K. Chen, and J. E. Beraun, Hot-Electron Blast "Induced by Ultrashort-Pulsed Lasers in Layered Media'', Int. J. Heat Mass Transfer, 45, (2002) 3369.
[11] Kurita, K. Komatsuzaki, and M. Hattoric, "Advanced material processing with nano- and femto-second pulsed laser, Int. J. Mach tool and Manuf''. 48, (2008) 220.
[12] S. W. Youn, M. Takahashi, H. Goto and R. Maeda, "Fabrication of micro-mold for glass embossing using focused ion beam, femtosecond laser, eximer laser and dicing techniques'', J. Mater. Process. Technol. 326, (2007) 187.
[13] Bonis, A. Galasso, V. Marotta, S. Orlando, A. Santagata, R. Teghil, S. Veronesi, P. Villani, A. Giardini, "Pulsed laser ablation of indium tin oxide in the nano and femtosecond regime: Characterization of transient species'', Appl. Surf. Sci. 252, (2006) 4632.
[14] J. K. Chen, D. Y. Tzou, and J. E. Beraun, "A semiclassical two-temperature model for ultrafast laser heating'', Int. J. Heat Mass Transfer. 49, (2006) 307.
[15] Y. Ho, K. M. Hung, M. Y. Wen, and J. E. Ho, "Thermal analysis of femtosecond laser processing for metal thin films'', Phys. Scr. T139, (2010) 014005.
[16] C. Y. Ho, M. Y. Wen, and C. S. Shih, "Parameter effects on temperatures in the thin film irradiated by ultrafast-pulse laser'', Int. J. Mod. Phys. B. 23, (2009) 1962.
[17] S. Sim, K. G. Kang, S. H. Lee, J. M. Kim and Y. E. Shin, A "Numerical Study on Nonequilibrium Heat Transfer and Crater Formation in Thin Metal Films Irradiated by Femtosecond Pulse Laser'', Mater. Sci. Forum. 580, (2008) 143.
[18] S. I. Anisimov, B. L. Kapeliovich and T. L. Perelman, "Electron emission from metal surfaces exposed to ultrashort laser pulses'', Sov. Phys. JETP. 39, (1974) 375.
[19] G. Kang, S. H. Lee, H. S. Ryou, Y. K. Choi, S. H. Park and J. S. Lee, "Wave Interference Effect in Thin Film Structures under Pulsed Laser Irradiation'', Mater. Trans. 49, (2008) 1880.
[20] K. Chen and J. E. Beraun, "Modeling of ultrashort laser ablation of gold films in vacuum'', J. Opt. A. Pure Appl. Opt. 5, (2003) 168.
[21] Eidmann, J. Meyer-ter-Vehn, T. Schlegel and S. Huller, "Hydrodynamic simulation of subpicosecond laser interaction with solid-density matter'', Phys. Rev. E. 62, (2000) 1202.
[22] Furusawa, K. Takahashi, H. Kumagai, K. Midorikawa and M. Obara, "Ablation characteristics of Au, Ag, and Cu metals using a femtosecond Ti:sapphire laser'', Appl. Phys. A. 69, (1999) 359.
[23] Jiang and H. L. Tsai, "Improved Two-Temperature Model for Femtosecond Laser Heating of Metal Thin Films'', J. Heat Transfer. 127, (2005) 1167.
[24] Q. Qui and C. L. Tien, "Heat transfer mechanisms during short-pulse laser heating on metals'', J. Heat Transfer. 115, (1993) 835.
[25] M. Saghebfar, M. K. Tehrani, S. M. R. Darbani and A. E. Majd, "Femtosecond pulse laser ablation of chromium: experimental results and two-temperature model simulations'', Appl. Phys. A. 123: 28, (2017) 1.
[26] M. L. Griffith, M. T. Ensz and D. E. Reckaway, "Femtosecond Laser Machining of Steel'', Proceedings of SPIE 4977, (2003) 118.
[27] M. I. Kaganov, I. M. Lifshitz and L. V. Tanatarov, "Relaxation between electrons and crystalline lattices'', Sov. Phys. JETP. 4, (1957) 173.
[28] J. K. Chen and J. E. Beraun, "Numerical study of ultrashort laser pulse interactions with metal films'', Numer. Heat Transfer A. 40, (2002) 1.
[29] T. Q. Qiu and C. L. Tien, Size efects on nonequilibrium laser heating of metal films, J. Heat Transfer. 115, (1993) 842.
[30] Welch, B.N. Hsu, A.C. Madison, R.B. Fair, "Low voltage electrowetting-on-dielectric platform using multi-layer insulators'', Sens. Actuators B Chem. 150, (2010) 465.
[31] Jo, M. Choe, C.Y. Cho, J.H. Kim, W. Park, S. Lee, W.K. Hong, T.W. Kim, S.J. Park, B.H. Hong, Y.H. Kahng, T. Lee, "Large-scale patterned multi-layer graphene films as transparent conducting electrodes for GaN light-emitting diodes'', Nanotech. 21, (2010) 175201.
[32] Kim, N.A. Charipar, A. Piqué, "Laser printing of multi-layered polymer/metal heterostructures for electronic and MEMS devices'', Appl. Phys. A. 99, (2010) 711.
[33] M. Lejman, V. Shalagatskyi, O. Kovalenko, T. Pezeril, V. V. Temnov and P. Ruello, "Ultrafast optical detection of coherent acoustic phonons emission driven by superdiffusive hot electrons'', J. Opt. Soc. Am. B. 31, (2014) 282.
[34] D. Brorson, J. G. Fujimoto and E. P. Ippen, "Femtosecond electronic heat-transport dynamics in thin gold films'', Phys. Rev. Lett. 59, (1987) 1962.
[35] V. V. Temnov, "Ultrafast acousto-magneto-plasmonics'', Nat. Photonics. 6, (2012) 728.
[36] S.I. Anisimov, B.L. Kapelovich and T.L. Perel'man, "Electron emission from metal surfaces exposed to ultra-short laser pulses'', Sov. Phys. JETP. 39, (1974) 375.
[37] Q. Qiu, T. Juhasz, C. Suarez, W. E. Bron, and C. L.Tien, "Femtosecond Laser Heating of Multi-Layer Metals-II Experiments'', Int. J. Heat Mass Transfer. 37, (1994) 2799.
[38] Li, D.M. Zhang, Z.H. Li, X.Y. Tan, R.Y. Fang, "Metal absorptivity in femtosecond pulsed laser ablation'', Front. Phys. China. 2, (2007) 322.
[39] Y.Q. Liu, J. Zhang, W.X. Liang, "Interaction of femtosecond laser pulses with metal photocathode'', Chin. Phys. Soc. 14, (2005) 1671.